

# Reducing molecular electronic Hamiltonian simulation cost for Linear Combination of Unitaries approaches

Ignacio Loaiza,<sup>1,2</sup> Alireza Marefat Khah,<sup>1,2</sup> Nathan Wiebe,<sup>3,4</sup> and Artur F. Izmaylov<sup>1,2</sup>

<sup>1</sup>*Chemical Physics Theory Group, Department of Chemistry, University of Toronto, Toronto, Canada*

<sup>2</sup>*Department of Physical and Environmental Sciences,  
University of Toronto Scarborough, Toronto, Canada*

<sup>3</sup>*Department of Computer Science, University of Toronto, Toronto, Canada*

<sup>4</sup>*Pacific Northwest National Laboratory, Richland, USA*

(Dated: February 14, 2023)

We consider different linear combination of unitaries (LCU) decompositions for molecular electronic structure Hamiltonians. Using these LCU decompositions for Hamiltonian simulation on a quantum computer, the main figure of merit is the 1-norm of their coefficients, which is associated with the quantum circuit complexity. It is derived that the lowest possible LCU 1-norm for a given Hamiltonian is half of its spectral range. This lowest norm decomposition is practically unattainable for general Hamiltonians; therefore, multiple practical techniques to generate LCU decompositions are proposed and assessed. A technique using symmetries to reduce the 1-norm further is also introduced. In addition to considering LCU in the Schrödinger picture, we extend it to the interaction picture, which substantially further reduces the 1-norm.

## I. INTRODUCTION

Quantum chemistry is often regarded as one of the most promising applications for quantum computers. The number of qubits required to represent the electronic states of a molecular Hamiltonian scales linearly with the number of orbitals, whereas an exponentially large number of classical bits is required [1, 2]; this is commonly known as the curse of dimensionality. In addition to be able to record the quantum wavefunction one needs to be able to prepare it. Over the last years, several quantum algorithms for efficient eigenstate state preparation have appeared, such as Quantum Phase Estimation [3, 4]. These algorithms require an implementation of the dynamical evolution operator  $e^{-i\hat{H}t}$  and the electronic structure Hamiltonian [5]

$$\hat{H} = \sum_{\sigma=\{\alpha,\beta\}} \sum_{ij}^N \tilde{h}_{ij} \hat{E}_{j\sigma}^{i\sigma} + \sum_{\sigma,\sigma'=\{\alpha,\beta\}} \sum_{ijkl}^N \tilde{g}_{ijkl} \hat{E}_{j\sigma}^{i\sigma} \hat{E}_{l\sigma'}^{k\sigma'}, \quad (1)$$

where  $\{\sigma, \sigma'\}$  are spin- $z$  projections,  $\{i, j, k, l\}$  are spacial orbitals,  $\tilde{h}_{ij}$  and  $\tilde{g}_{ijkl}$  are one- and two-electron integrals [43],  $N$  is the number of spacial one-electron orbitals, and  $\hat{E}_q^p \equiv \hat{a}_p^\dagger \hat{a}_q$  are single excitation operators (here and for the remainder of this work, we use the indices  $\{p, q, r, s\}$  to refer to spin-orbitals).

Implementing the time-evolution operator is a non-trivial task, known as the Hamiltonian simulation problem. This is usually done by decomposing the Hamiltonian into parts with favorable properties (e.g. fast-forwardable, unitary) [6], in approaches based on 1) Lie-Trotter-Suzuki formulas [7], 2) qubitization [8–10], 3) Dyson series [11], and 4) qDRIFT [10, 12, 13]. In all of these approaches, the decomposition method, together with the simulation method, define the necessary quantum resources for the simulation (i.e. number of gates and logical qubits). Some approaches, such as

those based on a Lie-Trotter-Suzuki expansion, do not require additional ancilla qubits, but can require significantly deeper circuits to achieve the same worst-case error bounds for non-local Hamiltonians [14, 15], whereas the tensor hypercontraction decomposition with a qubitization simulation yields the best gate provable complexity scaling to the best of our knowledge [10].

Even though the quantum cost of realizing the time-evolution operator has a complicated dependence such as the decomposition that is being used and the particular implementation of the simulation algorithm, the gate complexity of qubitization, LCU and qDRIFT can be shown to scale with respect to the 1-norm of the Hamiltonian decomposition into a linear combination of unitaries (LCU) [11, 16–19]  $\hat{H} = \sum_k u_k \hat{U}_k$ , namely  $\sum_k |u_k|$ . Thus minimizing this 1-norm of coefficients is vital for reducing the costs of a quantum simulation.

In this work, we focus on ways to decompose and transform the Hamiltonian such that the resulting 1-norm is minimized. We propose three approaches that can be used for lowering the 1-norm. The first builds the LCU's unitaries by grouping mutually anti-commuting Pauli products in the Hamiltonian after doing the fermion to qubit mapping [20], which either maintains or lowers the 1-norm and can be obtained efficiently using a sorted-insertion algorithm [21]. The second approach shifts the Hamiltonian by using symmetry operators; efficient linear programming routines for constructing the symmetry shift are also presented. Both of these approaches are of interest for any method which decomposes the Hamiltonian as an LCU. The third approach makes use of the interaction picture algorithm [16] combined with a Cartan sub-algebra (CSA) decomposition [22]. The basic idea is to separate the Hamiltonian into two fragments: a main one with an exponential that is straightforward to calculate, and a residual with a significantly smaller 1-norm; the main fragment is obtained using a greedy optimization routine that naturally minimizes the

1-norm of the residual. The Hamiltonian simulation is then performed by rotating the residual to the interaction picture frame. Simulating the residual, as shown in Ref. 16, will generally have a significantly lower cost than the full Hamiltonian simulation. The only caveat is that the residual becomes time-dependent in this new frame, requiring a time-dependent simulation method. Since only time-independent Hamiltonians can be simulated through qubitization, we use the Dyson series approach, which can also be used for time-dependent simulations while presenting an almost optimal scaling with respect to the 1-norm and simulation time [11, 16]. It is worth noting though that other approaches such as qDRIFT that has 1-norm scaling will also benefit from these optimizations [23].

This rest of the paper is organized as follows. We start by reviewing the Dyson series simulation method in Sec. IIA. A 1-norm lower bound theorem for LCU decompositions is then given in Sec. IIB, followed by an overview of different LCU decomposition strategies in Sec. IIC. A general methodology for reducing the simulation cost by using symmetries is shown in Sec. IID. Section IIE reviews the essential elements of the interaction picture method [16], along with our procedure for partitioning the Hamiltonian into two fragments. Once all the necessary methodologies have been introduced, our numerical results along with their discussion are shown in Sec. III.

## II. THEORY

### A. Hamiltonian simulation by LCU decomposition

An LCU decomposition for a Hamiltonian can be written as

$$\hat{H} = \gamma \hat{1} + \sum_k u_k \hat{U}_k, \quad (2)$$

where  $u_k$ 's are generally complex numbers, and  $\hat{U}_k$ 's are unitary operators. The identity shift can be trivially added or removed as a phase since  $e^{-i(\hat{H}+\gamma\hat{1})t} = e^{-i\hat{H}t}e^{-i\gamma t\hat{1}}$ , while still affecting the spectral norm of the Hamiltonian. The LCU in Eq.(2) has an associated 1-norm for coefficients of nontrivial unitaries

$$\lambda = \sum_k |u_k|. \quad (3)$$

The LCU decomposition allows one to construct a Hamiltonian oracle, a circuit that, with the usage of some ancilla qubits, is able to encode the action of  $\hat{H}$  on an arbitrary function  $|\psi\rangle$ . As shown in Fig. 1, the output of the oracle circuit contains a spurious remainder, which is made arbitrarily small through the subsequent use of amplitude amplification. The time-evolution operator  $e^{-i\hat{H}t}$  can always be expanded as a series: this expansion is

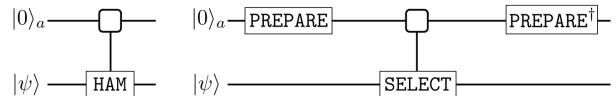


FIG. 1: Arbitrary Hamiltonian oracle (left) and LCU oracle (right) implementation by block-encoding, both with output  $|0\rangle_a \otimes \frac{\hat{H}}{\lambda} |\psi\rangle + |\text{remainder}\rangle$ .  $\text{PREPARE}|0\rangle_a = \sum_k \sqrt{\frac{u_k}{\lambda}} |k\rangle_a$  and  $\text{SELECT} = \sum_k |k\rangle\langle k|_a \otimes \hat{U}_k$  for the LCU shown in Eq.(2) and  $|k\rangle_a$  the  $k$ -th state of the ancilla register, requiring  $\lceil \log_2 M \rceil$  ancilla qubits, where  $M$  is the total number of unitaries in the LCU.

known as a Dyson series, which reduces to a Taylor series for the case where  $\hat{H}$  is time-independent.  $e^{-i\hat{H}t}$  is thus realized up to an arbitrary error  $\epsilon$  by implementing a truncated Dyson series using the amplitude amplified oracle circuit [11, 16, 24].

The cost of performing the Hamiltonian simulation with an error bound  $\epsilon$  scales in a linear, or nearly linear, manner with respect to the LCU's 1-norm [16], requiring

$$\mathcal{O}\left(\lambda t \text{ polylog} \frac{\lambda t}{\epsilon}\right) \quad (4)$$

applications of the oracle circuit for truncated Dyson simulation methods or

$$\mathcal{O}\left(\lambda t + \text{polylog} \frac{1}{\epsilon}\right), \quad (5)$$

using qubitization [25, 26]. The main aim of this work is to explore different ways in which we can reduce the 1-norm  $\lambda$ , lowering the quantum circuit depth/complexity of the Hamiltonian simulation.

### B. 1-norm bound

Let us start with a few general remarks on the minimum possible 1-norm and approaches for its minimization in practical LCU procedures for the electronic Hamiltonian.

**Theorem 1** (1-norm bound). *For a bounded hermitian operator  $\hat{H}$ , all its possible LCU decompositions have an associated 1-norm which is lower bounded by  $\Delta E/2 \equiv (E_{\max} - E_{\min})/2$ , where  $E_{\max}(E_{\min})$  is the highest (lowest) eigenvalue of  $\hat{H}$ .*

Formal proof of the theorem is given in Appendix A. A construction that achieves the minimum 1-norm follows from the following sequence of steps:

1. shift the Hamiltonian so that the largest and lowest eigenvalues become  $\pm(E_{\max} - E_{\min})/2$ :

$$\hat{H}_s = \hat{H} - \left(\frac{E_{\max} + E_{\min}}{2}\right) \hat{1} \quad (6)$$

2. obtain a rescaled Hamiltonian  $\hat{H}_{sr}$  such that  $\|\hat{H}_{sr}\| = 1$  (where  $\|\cdot\|$  is the spectral norm):

$$\hat{H}_{sr} = \frac{2\hat{H}_s}{E_{\max} - E_{\min}} \quad (7)$$

3. form the pair of unitaries:

$$\hat{U}_{\pm} = \hat{H}_{sr} \pm i\sqrt{\hat{1} - \hat{H}_{sr}^2}. \quad (8)$$

This procedure gives the LCU

$$\hat{H} = \left(E_{\min} + \frac{\Delta E}{2}\right) \hat{1} + \frac{\Delta E}{4} (\hat{U}_+ + \hat{U}_-), \quad (9)$$

with  $\Delta E/2$  its corresponding 1-norm.

The main problem of achieving this lowest 1-norm is the practical construction of  $\hat{U}_{\pm}$ ; for most molecular Hamiltonians they are highly multi-particle operators (i.e. including up to  $2N$ -electron excitations) because of the square-root in their definitions, and their calculation/implementation requires a complicated quantum singular value transformation to implement [26] the square-roots in an interval  $\|\hat{H}_{sr}\| \in [0, 1 - \delta]$  for some  $\delta > 0$ . Still, this theorem gives us a bound on the best achievable value for the 1-norm, which is useful to assess the quality of LCU decompositions.

### C. Unitary operators for LCU decompositions

In what follows we consider various practical forms of unitaries  $\hat{U}_k$  that appear when one is constructing an LCU representation for the electronic structure Hamiltonian [Eq. (1)].

#### 1. Pauli products

The simplest LCU decomposition uses the qubit representation of the Hamiltonian after it has been transformed from its fermionic representation by using one of the many available mappings (e.g. Jordan-Wigner and Bravyi-Kitaev transformations [27–31]):

$$\hat{H} = \sum_{k=1}^{N_p} c_k \hat{P}_k, \quad (10)$$

where  $\hat{P}_k$  are products of Pauli operators on different qubits,  $c_k$  are constants, and  $N_p$  is the total number of Pauli products. Since Pauli products are already unitary operators, Eq.(10) defines an LCU decomposition where the 1-norm is given by

$$\lambda^{(P)} = \sum_k |c_k|. \quad (11)$$

$\lambda^{(P)}$  can be related to electron integrals  $\tilde{h}_{ij}$  and  $\tilde{g}_{ijkl}$  as

$$\begin{aligned} \lambda^{(P)} = & \sum_{ij} \left| \tilde{h}_{ij} + 2 \sum_k \tilde{g}_{ijkk} \right| + \sum_{i>k,j>l} |\tilde{g}_{ijkl} - \tilde{g}_{ilkj}| \\ & + \frac{1}{2} \sum_{ijkl} |\tilde{g}_{ijkl}|. \end{aligned} \quad (12)$$

This relation is obtained using the Majorana representation for the Hamiltonian (detailed in Appendix B).

One way to improve  $\lambda^{(P)}$  is to apply orbital transformations  $\hat{U}_O$

$$\hat{U}_O(\vec{\theta}) = e^{\sum_{i>j} \theta_{ij} \sum_{\sigma} (\hat{E}_{j\sigma}^{i\sigma} - \hat{E}_{i\sigma}^{j\sigma})} \quad (13)$$

before transforming the Hamiltonian to qubit or Majorana representation [17],  $\hat{U}_O \hat{H} \hat{U}_O^\dagger$ . One can optimize the generator coefficients  $\theta_{ij}$  of orbital rotations in  $\hat{U}_O(\vec{\theta})$  with the 1-norm in Eq.(12) as the cost function.

#### 2. Grouping of anti-commuting Pauli products

Another way of reducing 1-norm of the Pauli product decomposition of the Hamiltonian [Eq. (10)] is via grouping of anti-commuting Pauli products[20]

$$\hat{H} = \sum_n a_n \hat{A}_n, \quad (14)$$

where

$$a_n = \sqrt{\sum_{i \in K_n} |c_i|^2}, \quad (15)$$

$$\hat{A}_n = \frac{1}{a_n} \sum_{k \in K_n} c_k \hat{P}_k, \quad (16)$$

$\hat{A}_n$  are linear combinations of anti-commuting Pauli products,  $\{\hat{P}_k, \hat{P}_{k'}\} = 2\delta_{kk'} \hat{1}$ , and  $\{K_n\}$  are groups of corresponding indices.

$\hat{A}_n$  are larger unitary transformations, and it can be shown that 1-norm of coefficients in Eq. (14) is always lower or equal than the 1-norm of the initial LCU decomposition: comparison of 1-norms for decompositions in Eqs. (10) and (14)

$$\lambda^{(AC)} = \sum_n |a_n| = \sum_n \sqrt{\sum_{i \in K_n} |c_i|^2} \quad (17)$$

$$\lambda^{(P)} = \sum_k |c_k| = \sum_n \sum_{i \in K_n} |c_i| \quad (18)$$

and using the triangle inequality for each  $K_n$ ,

$$\sum_{i \in K_n} |c_i| \geq \sqrt{\sum_{i \in K_n} |c_i|^2}, \quad (19)$$

proves that  $\lambda^{(\text{AC})} \leq \lambda^{(\text{P})}$ , where the equality takes place only for the trivial case where no grouping is made. Further note that from the Cauchy-Schwarz inequality

$$\sum_{i \in K_n} |c_i| \leq \sqrt{|K_n|} \sqrt{\sum_{i \in K_n} |c_i|^2}, \quad (20)$$

the gulf between these two bounds can be as much as a factor of  $\sqrt{|K_n|}$  suggesting that a substantial improvement can be attained in cases where the typical values of  $|K_n|$  seen are large.

Once the anti-commuting groups have been found, each unitary  $\hat{A}_n$  can be implemented as a product of unitaries:

$$\hat{A}_n = \prod_{k \in K_{n\uparrow}} e^{i\theta_k \hat{P}_k} \prod_{k \in K_{n\downarrow}} e^{i\theta_k \hat{P}_k}, \quad (21)$$

where the  $\uparrow(\downarrow)$  stands for ascending(descending) through  $K_n$ , and

$$\theta_k = \frac{1}{2} \arcsin \frac{c_k}{\sqrt{\sum_{i \in K_n, i \leq k} c_i^2}}. \quad (22)$$

### 3. Fermionic reflections

One can use fermionic operator algebra to construct an LCU decomposition. It is convenient to start with factorized decomposition of one- and two-electron terms of  $\hat{H}$  [Eq. (1)] introduced in double factorization (DF) method[8, 9] and the Cartan subalgebra approach (CSA)[22]

$$\hat{H}_1 = \sum_{\sigma=\{\alpha,\beta\}} \sum_{ij}^N \tilde{h}_{ij} \hat{E}_{j\sigma}^{i\sigma} \quad (23)$$

$$= \hat{U}_1 \left( \sum_{i\sigma} \lambda_{ii}^{(1)} \hat{n}_{i\sigma} \right) \hat{U}_1^\dagger \quad (24)$$

$$\hat{H}_2 = \sum_{\sigma,\sigma'=\{\alpha,\beta\}} \sum_{ijkl}^N \tilde{g}_{ijkl} \hat{E}_{j\sigma}^{i\sigma} \hat{E}_{l\sigma'}^{k\sigma'} \quad (25)$$

$$= \sum_{m=2}^M \hat{U}_m \left( \sum_{ij,\sigma\sigma'} \lambda_{ij}^{(m)} \hat{n}_{i\sigma} \hat{n}_{j\sigma'} \right) \hat{U}_m^\dagger, \quad (26)$$

where  $\hat{U}_m$  are orbital rotations as in Eq. (13),  $\hat{n}_p \equiv \hat{E}_p^p$  are the occupation number operators, and  $\lambda_{ij}^{(m)}$  are parameters of the decomposition. The difference between DF and CSA decompositions is in the rank of  $\lambda_{ij}^{(m)}$ ,  $m > 1$  matrices, DF has  $\lambda_{ij}^{(m)} = \epsilon_i^{(m)} \epsilon_j^{(m)}$  as an outer product of  $\epsilon_i^{(m)}$  vector, which makes  $\text{rank}(\lambda^{(m)}) = 1$ , while CSA does not have any restriction on the  $\lambda_{ij}^{(m)}$  rank.  $\hat{H}_2$  decompositions are truncated for fragments whose  $\lambda_{ij}^{(m)}$  are smaller than some threshold.

The convenience of these decompositions are in simplicity of transforming  $\hat{n}_p$  operators into reflections,[8–10]  $\hat{n}_p \rightarrow (2\hat{n}_p - \hat{1}) \equiv \hat{r}_p$ , where  $\hat{r}_p$  is the reflection on spin-orbital  $p$ . Accounting for idempotency and hermiticity of  $\hat{n}_p$ , one can easily check that  $\hat{r}_p^2 = 1$  and  $\hat{r}_p^\dagger = \hat{r}_p$ . Another important property of  $\hat{n}_p$ 's is their commutativity that allows one to transform the two-electron fragment in LCU

$$\hat{H}_2 \rightarrow \hat{H}_2^{(\text{LCU})} = \sum_{\sigma\sigma'} \sum_m \hat{U}_m \left( \sum_{ij} \frac{\lambda_{ij}^{(m)}}{4} \hat{r}_{i\sigma} \hat{r}_{j\sigma'} \right) \hat{U}_m^\dagger.$$

To use  $\hat{H}_2^{(\text{LCU})}$  as a part of the full Hamiltonian, the one-electron part requires the following adjustment

$$\hat{H}'_1 = \hat{H}_1 + 2 \sum_{\sigma} \sum_{ijk} \tilde{g}_{ijk} \hat{E}_{j\sigma}^{i\sigma}. \quad (27)$$

The modified one-electron operator can be decomposed as

$$\hat{H}'_1 = \hat{U}_1 \left( \sum_{\sigma,i} \mu_i \hat{n}_{i\sigma} \right) \hat{U}_1^\dagger, \quad (28)$$

where  $\mu_i$  are new parameters. Switching  $\hat{n}_p \rightarrow \hat{r}_p$  yields up to a constant shift

$$\hat{H}'_1 \rightarrow \hat{H}'_1^{(\text{LCU})} = \hat{U}_1 \left( \sum_{\sigma,i} \frac{\mu_i}{2} \hat{r}_{i\sigma} \right) \hat{U}_1^\dagger. \quad (29)$$

Thus, we have 1-norm  $\lambda^{(\text{F})} = \lambda_1 + \lambda_2$  associated with this LCU procedure, where  $\lambda_1$  ( $\lambda_2$ ) is 1-norm of  $\hat{H}'_1$  ( $\hat{H}_2^{(\text{LCU})}$ )

$$\lambda_1 = \sum_i |\mu_i|, \quad (30)$$

$$\begin{aligned} \lambda_2 &= \frac{1}{4} \sum_m \sum_{\substack{\sigma\sigma',ij \\ i\sigma \neq j\sigma'}} |\lambda_{ij}^{(m)}| \\ &= \sum_m \sum_{ij} |\lambda_{ij}^{(m)}| - \frac{1}{2} \sum_m \sum_i |\lambda_{ii}^{(m)}|, \end{aligned} \quad (31)$$

Note that the obtained fermionic LCU decomposition can be transformed to a qubit LCU form using any fermion-qubit mappings.

### 4. Square-root unitarization technique

Another way to transform the quadratic polynomials

$$\hat{f}^{(m)} = \sum_{ij,\sigma\sigma'} \lambda_{ij}^{(m)} \hat{n}_{i\sigma} \hat{n}_{j\sigma'} \quad (32)$$

into unitaries is via steps described in Theorem 1. This procedure gives the lowest 1-norm for LCU of each fragment. First, we shift and rescale each fragment so that

their eigenvalues are in the interval  $[-1, 1]$  (i.e.  $\hat{f}^{(m)} \rightarrow \hat{f}_{sr}^{(m)}$ , as seen in Eqs.(6,7)). Second, unitary operators can be defined for each fragment as

$$\hat{V}_m^{(\pm)} = \hat{f}_{sr}^{(m)} \pm i\sqrt{\hat{1} - (\hat{f}_{sr}^{(m)})^2}. \quad (33)$$

This leads to the LCU of the two-electron Hamiltonian up to a constant as

$$\hat{H}_2^{(\text{LCU})} = \sum_{m=2}^M \frac{\|\hat{f}^{(m)}\|_{\Delta}}{2} \hat{U}_m (\hat{V}_m^{(+)} + \hat{V}_m^{(-)}) \hat{U}_m^{\dagger}, \quad (34)$$

where  $\|\hat{f}^{(m)}\|_{\Delta} \equiv f_{\max}^{(m)} - f_{\min}^{(m)}$  is a spectral range of  $\hat{f}^{(m)}$  and  $f_{\max(\min)}^{(m)}$  is the maximum (minimum) eigenvalue of fragment  $\hat{f}^{(m)}$ . The corresponding 1-norm is

$$\lambda_2^{(sr)} = \frac{1}{2} \sum_m \|\hat{f}^{(m)}\|_{\Delta}, \quad (35)$$

In general, the explicit construction and implementation of  $\hat{V}_m^{(\pm)}$  unitaries becomes prohibitively expensive as the number of orbitals grows, as the square-root function includes all possible products of the occupation numbers. Using a different scaling such that  $\|\hat{f}_{sr}^{(m)}\| \leq 1 - \delta$ , this unitary operator can be approximated within error  $\epsilon$  using  $O((\frac{1}{\delta}) \log(1/\epsilon))$  invocations of the fragment  $\hat{f}^{(m)}$  [26]. Nevertheless, given the complexity of implementing such circuits, the square-root unitarization is primarily used as a lower bound of the 1-norm for fermionic decompositions.

This procedure can also be done for the one-electron term  $\hat{H}_1'$  (Eq.(28)), obtaining

$$\lambda_1^{(sr)} = \left( \sum_{\mu_i > 0} \mu_i - \sum_{\mu_i < 0} \mu_i \right) = \sum_i |\mu_i|. \quad (36)$$

We note that this 1-norm is the same as that in Eq.(30). This shows that, using the fermionic LCU decomposition in Eq. (28) gives the LCU with the lowest possible 1-norm for the one-electron part since its 1-norm coincides with that in the square-root approach.

### 5. Chebyshev complete-square block-encoding:

The relation  $\lambda_{ij}^{(m)} = \epsilon_i^{(m)} \epsilon_j^{(m)}$  in the double factorization approach allows one to factorize quadratic polynomials into complete squares

$$\hat{f}^{(m)} = \sum_{ij, \sigma\sigma'} \lambda_{ij}^{(m)} \hat{n}_{i\sigma} \hat{n}_{j\sigma'} = \left( \sum_{i, \sigma} \epsilon_i^{(m)} \hat{n}_{i\sigma} \right)^2. \quad (37)$$

Given a fragment with a complete-square structure  $\hat{f} = \hat{l}^2$ , its implementation can be efficiently done in two steps.

First, we transform  $\hat{l}$  into an LCU by the mapping  $\hat{n}_p \rightarrow \hat{t}_p$ :

$$\hat{l} = \left( \sum_i \epsilon_i \right) \hat{1} + \sum_i \frac{\epsilon_i}{2} \sum_{\sigma} \hat{t}_{i\sigma}. \quad (38)$$

The corresponding 1-norm of this LCU becomes  $\sum_i |\epsilon_i| \equiv \lambda_l$ , which as shown by Eq.(36) is optimal. Second, the qubitization technique [8, 25] is used for block-encoding  $\hat{f}$ . This is done by implementing the Chebyshev polynomial  $T_2[\hat{l}_n] = 2\hat{l}_n^2 - \hat{1}$ , with  $\hat{l}_n \equiv \frac{\hat{l}}{\lambda_l}$ . Thus, by presenting

$$\hat{f} = \frac{\lambda_l^2}{2} T_2[\hat{l}_n] + \frac{\lambda_l^2}{2} \hat{1}, \quad (39)$$

this fragment can be implemented with an associated 1-norm cost of  $\frac{\lambda_l^2}{2}$ . We will refer to this technique as a complete-square encoding. Note that the implementation of  $\hat{l}$  as an LCU is done without the constant shift appearing in Eq.(38). This shift appears as a one-body correction when implementing  $\hat{f}$  through the complete-square encoding. As demonstrated in Ref.10, the adjusted one-electron Hamiltonian in Eq.(27) can be recovered by adding the one-body corrections from all fragments in the two-electron Hamiltonian  $\hat{H}_2$ . Constant terms must also be accounted for and can be trivially added after representing  $\hat{H}$  as an LCU.

Finally, we note that the 1-norm obtained for  $\hat{f}$  through the square-root decomposition is the same as that obtained through the complete-square encoding. The 1-norm for the two-body part of  $\hat{f}^{(m)}$  becomes

$$\lambda_2^{(m)} = \frac{1}{2} \left( \sum_i |\epsilon_i^{(m)}| \right)^2. \quad (40)$$

Thus, complete-square fragments can be encoded optimally with the lowest possible 1-norm, while for the more general case of  $\lambda_{ij}^{(m)} \neq \epsilon_i^{(m)} \epsilon_j^{(m)}$  either the square-root technique can be applied or their  $\lambda_{ij}^{(m)}$  can be decomposed into a sum over complete squares.

### D. Norm reduction by using symmetry shifts

The idea of symmetry shifts  $\hat{S}$  uses the same rationale as that of shifting the Hamiltonian by  $\gamma\hat{1}$ : the overall 1-norm of the LCU decomposition can be lowered by decomposing  $\hat{H} - \hat{S}$  instead of  $\hat{H}$ . By considering an arbitrary symmetry operator  $\hat{S}$  for which  $[\hat{H}, \hat{S}] = 0$ , the time-evolution operator becomes

$$e^{-i\hat{H}t} = e^{-i\hat{S}t} e^{-i(\hat{H}-\hat{S})t}. \quad (41)$$

For a wavefunction that obeys symmetry constraints,  $e^{-i\hat{S}t}$  only introduces a phase, making the simulation problem equivalent to the simulation of  $\hat{H} - \hat{S}$ . In this section we focus on ways to find this shift operator such that

the 1-norm of the resulting LCU is lowered. Note that this symmetry shift technique can also improve Trotter methods as well.

$\hat{S}$  can be built by an arbitrary function  $f(\{\hat{S}_u\})$  over a set of symmetries  $\mathbb{S} = \{\hat{S}_u\}$  satisfying the conditions  $[\hat{S}_u, \hat{S}_v] = [\hat{S}_u, \hat{H}] = 0, \forall u, v \in 1, \dots, |\mathbb{S}|$ . The symmetries  $\mathbb{S}$  can be selected from existing molecular symmetries, such as the electron number operator  $\hat{N}_e$ , the z-projection of electron spin  $\hat{S}_z$ , the total electronic spin  $\hat{S}^2$ , and molecular point group symmetries. However, in this study we restrict the pool of symmetries to  $\mathbb{S} = \{\hat{N}_e\}$ . This choice preserves the Hamiltonian structure in Eq.(1) where the fermionic tensors  $\tilde{h}_{ij}$  and  $\tilde{g}_{ijkl}$  run over spacial orbitals instead of spin-orbitals. There are three benefits to this structure: (1) all LCU methodologies can be used without modification, (2) it allows for efficient compilation of LCU unitaries on a quantum computer[10], and (3) it improves the efficiency of storage and manipulation of these tensors on a classical computer.

The symmetry shift procedure contains two steps. First, the optimal shift for the two-electron operator is found, such that the 1-norm of  $\hat{H}_2(s_2) \equiv \hat{H}_2 - s_2 \hat{N}_e^2$  is minimized. Second, the modified one-body Hamiltonian  $\hat{H}'_1(s_2)$  is obtained [Eq. (27)] and the 1-norm of  $\hat{H}'_1(s_2) - s_1 \hat{N}_e$  is minimized, yielding  $\hat{S} = s_1 \hat{N}_e + s_2 \hat{N}_e^2$ . This procedure reduces 1-norm of  $\hat{H} - \hat{S}$ , while preserving the  $\hat{H}$  structure so that all LCU methodologies can be applied. Efficient routines for finding  $s_1$  and  $s_2$  are detailed in Appendix C 1.

### E. Hamiltonian simulation in the interaction picture

Here, we consider the interaction picture Hamiltonian simulation introduced in Ref. 16. The Hamiltonian is split in two fragments,  $\hat{H} = \hat{H}_0 + \hat{H}_R$ , where  $\hat{H}_0$  is exactly solvable or fast-forwardable and  $\hat{H}_R$  is a residual part. It is beneficial to achieve  $\|\hat{H}_0\| \gg \|\hat{H}_R\|$  in this splitting. The simulation of the molecular Hamiltonian then requires the time-dependent simulation of the residual Hamiltonian in the interaction picture, which reduces the overall cost of the simulation.

For selecting  $\hat{H}_0$  we use the CSA approach, by finding the orbital rotation amplitudes  $\vec{\theta}$  and occupation number parameters  $(\vec{\mu}, \vec{\lambda})$  in

$$\hat{H}_0 = \hat{U}(\vec{\theta}) \left( \sum_{\sigma,i} \mu_i \hat{n}_{i\sigma} + \sum_{\sigma\sigma',i>j} \lambda_{ij} \hat{n}_{i\sigma} \hat{n}_{j\sigma'} \right) \hat{U}^\dagger(\vec{\theta}), \quad (42)$$

to minimize  $\|\hat{H} - \hat{H}_0\|$ , where the norm is defined as a sum of  $L_2$  norms for one- and two-electron tensors.  $\hat{H}_0$  corresponds to a largest mean-field solvable part[32] of  $\hat{H}$ .

In the interaction picture, the time-dependent

Schrödinger equation is

$$i\partial_t |\psi_I(t)\rangle = \hat{H}_R^{(I)}(t) |\psi_I(t)\rangle, \quad (43)$$

where  $|\psi_I(t)\rangle \equiv e^{i\hat{H}_0 t} |\psi(t)\rangle$  and

$$\hat{H}_R^{(I)}(t) = e^{i\hat{H}_0 t} \hat{H}_R e^{-i\hat{H}_0 t}. \quad (44)$$

Simulating the evolution under the full Hamiltonian is thus equivalent to rotating to the interaction frame by  $e^{i\hat{H}_0 t}$ , doing the simulation with the time-dependent residual  $\hat{H}_R^{(I)}(t)$ , and rotating back to the Schrödinger frame by  $e^{-i\hat{H}_0 t}$ .

As shown in Ref. 16, the associated simulation cost for the interaction picture method using a truncated Dyson series is

$$\mathcal{O} \left( \lambda_R t \text{polylog} \left( \frac{\lambda t}{\epsilon} \right) \right) \quad (45)$$

applications of the  $\hat{H}_R$  Hamiltonian oracle and of  $e^{i\tau\hat{H}_0}$  (with different values of  $\tau$ ), where  $\lambda_R$  is the 1-norm of the LCU decomposition of  $\hat{H}_R$ .

## III. RESULTS AND DISCUSSION

### A. Schrödinger picture

Table I shows the 1-norms obtained for different methods on molecular Hamiltonians. A comparison of each method was made with respect to the simple Pauli product decomposition. The linear fit for each LCU decomposition was done by associating to each molecule two coordinates:  $x$  is the 1-norm of the Pauli product LCU, and  $y$  is the 1-norm of the considered LCU method. The slope of the linear fit quantifies the average 1-norm reduction of each method with respect to the Pauli product LCU decomposition. Note that here we do not obtain the scaling of 1-norm with respect to the system size. Such a scaling consideration would require a more systematic approach to increasing the system size and is left for future studies.

For the qubit-based methods, the orbital optimization scheme presents an improvement with respect to the Pauli product LCU, as expected from the analysis in Ref. 17. This trend is also true for the anti-commuting grouping technique, and the most significant improvement was obtained when combining both techniques. Symmetry shift presented a significant improvement in 1-norm for all systems. It is the best qubit-based method when combined with the anti-commuting grouping and orbital optimization techniques, with an average decrease of 1-norm by 57%.

Before discussing the fermionic methods, we would like to emphasize that complete-square encoding will yield the lowest possible 1-norm for fragments with

System	Symmetry shift	$\Delta E/2$	Pauli	OO-Pauli	AC	OO-AC	DF	GCSA-F	GCSA-SR
H <sub>2</sub>	–	0.82	1.58(4)	1.58(4)	1.49(4)	1.49(4)	1.37(2)	1.77(4)	1.37(2)
	yes	0.66	0.84(4)	0.84(4)	0.79(5)	0.79(5)	0.75(2)	0.84(4)	0.74(2)
LiH	–	4.93	13.0(10)	12.4(11)	10.2(7)	10.2(8)	9.34(5)	11.0(11)	8.25(5)
	yes	3.57	7.62(10)	7.02(10)	5.13(7)	5.03(7)	4.76(5)	5.48(11)	4.61(5)
BeH <sub>2</sub>	–	9.99	22.8(10)	21.9(12)	18.0(8)	17.9(10)	16.4(5)	20.1(12)	14.6(5)
	yes	7.31	14.2(10)	13.0(12)	10.2(8)	9.83(8)	9.77(5)	11.5(11)	9.58(5)
H <sub>2</sub> O	–	41.9	71.9(11)	60.1(12)	57.2(8)	55.7(9)	53.7(5)	59.2(12)	50.6(5)
	yes	28.9	46.0(11)	37.7(12)	34.4(8)	32.9(9)	32.7(5)	36.1(12)	31.9(5)
NH <sub>3</sub>	–	33.8	68.6(12)	54.5(12)	48.8(9)	46.8(12)	44.7(6)	50.6(13)	40.6(6)
	yes	23.1	46.3(12)	34.6(12)	29.8(9)	27.8(12)	28.1(6)	31.8(13)	26.5(6)
Linear fit slope	–	0.53±0.03	1	0.83±0.02	0.76±0.02	0.73±0.02	<b>0.70±0.02</b>	0.79±0.02	0.65±0.03
	yes	0.37±0.02	0.65±0.01	0.52±0.01	0.46±0.01	<b>0.43±0.01</b>	<b>0.43±0.01</b>	0.48±0.01	0.42±0.01

TABLE I: 1-norms for molecular Hamiltonian using different LCU decompositions:  $\Delta E/2 = (E_{\max} - E_{\min})/2$  is the lowest 1-norm possible; Pauli, Pauli products; AC, anti-commuting Pauli product grouping; OO-Pauli, Pauli products with orbital optimization for 1-norm; AC-OO, orbital optimization scheme with subsequent anti-commuting Pauli product grouping; DF, double factorization; GCSA, Greedy CSA decomposition. Symmetry shift procedure is outlined in Sec. II D. Suffixes -F and -SR for GCSA correspond to fermionic unitarization and square-root unitarization techniques, respectively. DF results correspond to complete-square technique, which yield a minimal 1-norm. Values in parenthesis represent  $\lceil \log_2(\# \text{ unitaries}) \rceil$ , which is associated with the necessary number of ancilla qubits and circuit depth (see Refs.9, 10 for a more detailed discussion). A cut-off threshold of  $10^{-6}$  was used for counting unitaries in fermionic unitarizations. The linear fit was obtained by associating to each molecule two coordinates:  $x$  is the 1-norm of the Pauli product LCU, and  $y$  is the 1-norm of the considered LCU method. The slope of the linear regression is given with the associated standard error ( $\pm$ ). Highlights show methods with best scaling that are viable to implement on a quantum computer.

System	$\Delta E/2$	Pauli	OO-Pauli	AC	OO-AC	DF	GCSA-F	GCSA-SR
H <sub>2</sub>	0.20	0.30(3)	0.30(3)	0.30(3)	0.30(3)	0.20(1)	0.30(3)	0.20(1)
LiH	0.80	3.13(10)	2.88(10)	1.50(7)	1.49(7)	1.40(5)	2.12(11)	1.53(5)
BeH <sub>2</sub>	1.00	5.78(10)	4.41(10)	2.60(8)	2.33(8)	2.89(5)	3.95(12)	2.44(5)
H <sub>2</sub> O	2.38	9.18(11)	7.77(11)	4.32(8)	3.91(8)	4.47(5)	7.94(12)	5.34(6)
NH <sub>3</sub>	3.01	14.3(13)	11.2(13)	5.86(10)	5.23(10)	6.09(6)	10.2(13)	6.42(6)
Linear fit slope	0.039±0.003	0.172±0.022	0.139±0.016	0.075±0.008	<b>0.067±0.007</b>	0.078±0.009	0.131±0.085	0.085±0.006

TABLE II: Same as Table I, but for residual Hamiltonian  $\hat{H}_R$ . The linear fit is calculated with respect to the Pauli product LCU for  $\hat{H}$ .

a complete-square structure. Therefore, the optimal 1-norms also correspond to those of DF with complete-square encoding (used in Refs. 9, 10). We also note that implementing fragments as a single unitary not only reduces the 1-norm, but also the number of unitaries and consequently the number of ancilla qubits. Thus, the square-root technique works as a lower bound for the 1-norm and can be used to know how much the fermionic LCU can be further improved along with providing intuition about the minimal number of ancillary qubits needed. Since the number of ancilla qubits will also depend on the particular implementation of the controlled unitaries [9, 10], Table I shows  $\lceil \log_2 M \rceil$ , where  $M$  is the number of unitaries in the LCU and the number of ancillas scales with  $\mathcal{O}(\lceil \log_2 M \rceil)$ .

As shown in Table I, all fermionic methods show a significant improvement with application of symmetry shift. The symmetry-shifted greedy CSA approach with the square-root technique (GCSA-SR) gave lowest 1-norms, with an average reduction of 58%. However, this is an unattainable lower bound. Thus, we highlight methods

with the best average gain that use viable implementation methods by employing simple quantum circuits. Before symmetry shift, the best fermionic method is DF, having an average decrease of the 1-norm by 30%. When the symmetry shift was applied, all methods presented a significant improvement, having the largest reduction of 57% for DF.

Even though the CSA decomposition is a more general ansatz than DF, the greedy algorithm used in CSA for finding the fragments is heuristic and sacrifices some flexibility of a full optimization in exchange for computational efficiency. This makes the number of fragments and as a result the number of ancilla qubits appearing in GCSA larger than those in DF.

It should also be noted that doing the GCSA decomposition is a computationally expensive process compared to DF; these methods respectively require a non-linear optimization and a Cholesky decomposition. When considering the symmetry shift, both anti-commuting with orbital optimization and DF with a fermionic unitarization methods present the best improvement for 1-norm while having the lowest classical pre-processing cost.

Both these methods show an improvement of 57%, offering a significant improvement over all methods without symmetry shift.

Although both DF and CSA decompositions could be done over the full Hamiltonian by representing it as a single two-electron operator (see Appendix B), separating the one- and two-electron terms yields a very significant improvement of the 1-norm, while also allowing for manipulations to be done directly on spacial orbitals (as opposed to spin-orbitals), which greatly lowers the classical pre-processing cost of the decompositions.

Finally, we discuss how our results compare to the 1-norm lower bound  $\Delta E/2$ . When not considering symmetry shift, DF lowered the 1-norm by 30% of the possible reduction, while with symmetry shift it captured 57%. When dealing with symmetry shifted molecular Hamiltonians, both DF and the orbital-optimized anti-commuting grouping obtain a 1-norm that is very close to the lower bound along a small number of required ancilla qubits, placing them as almost optimal decomposition methods.

## B. Interaction picture

Table II provides results for the same LCU method but in the interaction picture. The linear fit results are also obtained by comparing the 1-norms with respect to the Pauli product LCU 1-norm of the molecular Hamiltonian in the Schrödinger picture.

Here, performing the symmetry shift does not yield any significant improvements on any of the methods and thus is not shown in Table II. This can be attributed to an implicit inclusion of any symmetry shift of  $\hat{H}_0$  in its  $\mu_i$  and  $\lambda_{ij}$  coefficients:  $\hat{H}_0 - \sum_u s_u \hat{S}_u \equiv \hat{U}(\vec{\theta}) \left( \sum_{\sigma,i} \tilde{\mu}_i(\vec{s}) \hat{n}_{i\sigma} + \sum_{\sigma\sigma',i>j} \tilde{\lambda}_{ij}(\vec{s}) \hat{n}_{i\sigma} \hat{n}_{j\sigma'} \right) \hat{U}^\dagger(\vec{\theta})$  since  $[\hat{S}_u, \hat{U}(\vec{\theta})] = 0$  and  $\hat{S}_u$  is a polynomial of occupation numbers. The DF technique is the most optimal fermionic method, with an average 1-norm decrease of 92% with respect to the Pauli product LCU of the molecular Hamiltonian. Surprisingly, the results from GCSA are not consistently better than those of DF. We attribute this to the heuristic nature of the greedy optimization. DF is thus a better alternative than GCSA for decomposing  $\hat{H}_R$ , presenting a greater 1-norm reduction, smaller number of fragments, and a lower classical pre-processing cost.

For the qubit-based methods, the anti-commuting grouping presented the greatest 1-norm reduction. We observed that applying the orbital optimization scheme further improved the results when combined with the anti-commuting grouping. The combination of these techniques yielded an average 1-norm reduction of 93%, while without the orbital optimization scheme the anti-commuting grouping presented an average decrease of

92%.

## IV. CONCLUSION

We have presented a wide set of techniques for performing the LCU decomposition of molecular Hamiltonians, using the associated 1-norm of the decomposition as the main figure of merit. The greatest 1-norm reduction was observed for the interaction picture methodology combined with the orbital optimization scheme and anti-commuting Pauli products grouping, with an average 1-norm decrease of 93% with respect to the Pauli product LCU of the molecular Hamiltonian  $\hat{H}$ . All methods that work with the residual  $\hat{H}_R$  of the interaction picture greatly improved the performance over decomposing  $\hat{H}$ , decreasing the 1-norm by an order of magnitude. However, the interaction picture methodology requires a time-dependent simulation method, rendering it incompatible with some simulation techniques such as qubitization (although recent work has shown that qubitization can be made to work for restricted families of time-dependent Hamiltonians, existing results preclude the interaction picture [33]). For the time-independent case, the symmetry shift technique here introduced can be employed, which yields a significant decrease of the 1-norm when compared with commonly used techniques [9] and can be included in a tensor hypercontraction framework [10]. Even though we only used symmetry shifts that can be written as functions of occupation number operators such as  $\hat{N}_e$  and  $\hat{S}_z$ , the results presented here provide an incentive for exploring more symmetries with different structures, such as  $\hat{S}^2$  and molecular point group symmetries. Finally, we have found tight bounds for the 1-norm of an arbitrary LCU, with the most efficient decomposition shown here being close to the lower bound.

Overall, we presented different methodologies for reducing the LCU 1-norm cost of molecular Hamiltonians, with significant improvements that can be applied both for time-independent [8] and time-dependent [11, 16] simulation methods. We expect our results to be of use for any methodology that uses LCU decomposition of molecular Hamiltonians.

## Acknowledgements

I.L. is grateful to Tzu-Ching Yen for helpful discussions and to Luis Martínez-Martínez, Joshua T. Cantin, and Seonghoon Choi for their comments on the manuscript, and is supported by the funding of the Anoush Khoshkish Graduate Research Scholarship in Chemistry. A.F.I. acknowledges financial support from the Google Quantum Research Program, Zapata Computing, and the Natural Sciences and Engineering Research Council of Canada. N.W. acknowledges funding from the Google Quantum



Research Program, the Natural Sciences and Engineering Research Council of Canada and N.W.'s theoretical work on this project was supported by the U.S. Department of Energy, Office of Science, National Quantum Information Science Research Centers, Co-Design Center for Quantum Advantage under contract number DE-SC0012704.

### Appendix A: Proof of the lowest 1-norm theorem

**Theorem 1** (1-norm bound). *For a bounded hermitian operator  $\hat{H}$ , all its possible LCU decompositions have an associated 1-norm which is lower bounded by  $\Delta E/2 \equiv (E_{\max} - E_{\min})/2$ , where  $E_{\max}(E_{\min})$  is the highest (lowest) eigenvalue of  $\hat{H}$ .*

The construction of an LCU that achieves the lower bound is given in Sec. IIB of the main text. We now proceed to show, by contradiction, that no LCU with a lower 1-norm can be found.

*Proof of Theorem 1.* Let us assume that it is possible to construct  $\hat{H} = \sum_k u_k \hat{U}_k$  such that  $\sum_k |u_k| < \Delta E/2$ . Denoting  $|\psi_{\max}\rangle(|\psi_{\min}\rangle)$  the maximum(minimum) eigenvectors, we have

$$\begin{aligned} \langle \psi_{\max} | \sum_k u_k \hat{U}_k | \psi_{\max} \rangle &= E_{\max} \\ \langle \psi_{\min} | \sum_k u_k \hat{U}_k | \psi_{\min} \rangle &= E_{\min}. \end{aligned} \quad (\text{A1})$$

We therefore have that  $\Delta E/2$  can be bounded above by

$$\begin{aligned} \frac{\Delta E}{2} &= \frac{1}{2} \left( \langle \psi_{\max} | \sum_k u_k \hat{U}_k | \psi_{\max} \rangle - \langle \psi_{\min} | \sum_k u_k \hat{U}_k | \psi_{\min} \rangle \right) \\ &\leq \sum_k |u_k| < \frac{\Delta E}{2}, \end{aligned} \quad (\text{A2})$$

where we have used the triangle inequality and the fact that  $|\langle \psi | \hat{U} | \psi \rangle| \leq 1$  for any unitary  $\hat{U}$  and wavefunction  $|\psi\rangle$ . This is a contradiction, thus  $\sum_k |u_k| \geq \Delta E/2$  as claimed.  $\square$

### Appendix B: One-electron term transformations

Due to idempotency of occupation operator terms,  $(\hat{E}_{i\sigma}^{i\sigma})^2 = \hat{E}_{i\sigma}^{i\sigma}$ , one-electron terms can be transformed to two-electron terms and vice versa. This section shows how these transformations can be done for general two-electron operators.

#### 1. Transforming to two-electron terms

We start by showing how to combine one- and two-electron terms into a sum of two-electron terms. An arbitrary operator with spin-orbit symmetry can be written

as

$$\hat{O} = \hat{O}_1 + \hat{O}_2 \quad (\text{B1})$$

$$= \sum_{\sigma} \sum_{ij} o_{ij} \hat{E}_{j\sigma}^{i\sigma} + \sum_{\sigma\sigma'} \sum_{ijkl} o_{ijkl} \hat{E}_{j\sigma}^{i\sigma} \hat{E}_{l\sigma'}^{k\sigma'}. \quad (\text{B2})$$

We note that each  $o_{ij}$  is multiplied by two excitation operators  $\hat{E}_{j\sigma}^{i\sigma}$  with  $\sigma \in (\alpha, \beta)$ , while each  $o_{ijkl}$  is multiplied by four operators  $(\alpha\alpha, \alpha\beta, \beta\alpha, \beta\beta)$ . Because of this, combining both operators requires to change from a (spacial) orbital representation into the spin-orbital one; the combined two-electron operator will have different components for  $(\alpha\alpha, \beta\beta)$  and  $(\alpha\beta, \beta\alpha)$ . We now transform the one-electron term into a two-electron operator, noting that several different transformations can be done here. We use the one that maintains a symmetric two-electron tensor since this property makes computational manipulations more efficient:

$$\hat{O}_1 = \hat{U} \sum_{\sigma} \sum_i \mu_i \hat{n}_{i\sigma} \hat{U}^{\dagger} \quad (\text{B3})$$

$$= \hat{U} \sum_{\sigma} \sum_i \mu_i \hat{n}_{i\sigma} \hat{n}_{i\sigma} \hat{U}^{\dagger} \quad (\text{B4})$$

$$= \sum_{\sigma} \sum_{ijkl} \tilde{o}_{ijkl} \hat{E}_{j\sigma}^{i\sigma} \hat{E}_{l\sigma}^{k\sigma}, \quad (\text{B5})$$

with

$$\tilde{o}_{ijkl} = \sum_m \mu_m U_{im} U_{jm} U_{km} U_{lm}, \quad (\text{B6})$$

for  $\hat{U} \equiv \sum_{\sigma} \sum_{ij} U_{ij} \hat{E}_{j\sigma}^{i\sigma}$ . The combined two-electron tensor is  $o_{pqrs}$ , where

$$\hat{O} = \sum_{\sigma} \sum_{ijkl} (\tilde{o}_{ijkl} + o_{ijkl}) \hat{E}_{j\sigma}^{i\sigma} \hat{E}_{l\sigma}^{k\sigma} + \sum_{\sigma \neq \sigma'} \sum_{ijkl} o_{ijkl} \hat{E}_{j\sigma}^{i\sigma} \hat{E}_{l\sigma'}^{k\sigma'} \quad (\text{B7})$$

$$\equiv \sum_{pqrs} o_{pqrs} \hat{E}_q^p \hat{E}_s^r. \quad (\text{B8})$$

#### 2. Separating one-electron terms

Here we show how one-electron terms can be separated from the two-electron tensor, which is used to connect the fermionic and qubit representations. This is necessary for writing the 1-norm of qubit-based methods as a function of the molecular integrals, and also for a more efficient sorted-insertion algorithm that does not require any fermion to qubit mappings. This methodology is introduced in Ref. 17, only the final result and key steps are presented here. We start from a general two-electron operator with spin-symmetry, as seen in Eq.(B2). For the next step, we switch to the Majorana representation, where fermionic operators are mapped into Majorana operators as

$$\hat{\gamma}_{j\sigma,0} = \hat{a}_{j\sigma} + \hat{a}_{j\sigma}^{\dagger} \quad (\text{B9})$$

$$\hat{\gamma}_{j\sigma,1} = -i(\hat{a}_{j\sigma} - \hat{a}_{j\sigma}^{\dagger}), \quad (\text{B10})$$

which have the well-known algebraic relations:

$$\{\hat{\gamma}_{p,n}\hat{\gamma}_{q,m}\} = 2\delta_{pq}\delta_{nm}\hat{1} \quad (\text{B11})$$

$$\hat{\gamma}_{p,n}^\dagger = \hat{\gamma}_{p,n} \quad (\text{B12})$$

$$\hat{\gamma}_{p,n}^2 = \hat{1}, \quad (\text{B13})$$

for  $n, m = 0, 1$ . By transforming the fermionic operators into Majoranas, after proper manipulations,  $\hat{O}$  can be written as

$$\begin{aligned} \hat{O} = & \left( \sum_i o_{ii} + \frac{1}{2} \sum_{ij} o_{ijji} + \sum_{ij} o_{ijjj} \right) \hat{1} \\ & + \frac{i}{2} \sum_{\sigma} \sum_{ij} \left( o_{ij} + 2 \sum_k o_{ijkk} \right) \hat{\gamma}_{i\sigma,0} \hat{\gamma}_{j\sigma,1} \\ & - \frac{1}{4} \sum_{\sigma \neq \sigma'} \sum_{ijkl} o_{ijkl} \hat{\gamma}_{i\sigma,0} \hat{\gamma}_{j\sigma,1} \hat{\gamma}_{k\sigma',0} \hat{\gamma}_{l\sigma',1} \\ & - \frac{1}{2} \sum_{\sigma} \sum_{i>k,l>j} (o_{ijkl} - o_{ilkj}) \hat{\gamma}_{i\sigma,0} \hat{\gamma}_{j\sigma,1} \hat{\gamma}_{k\sigma,0} \hat{\gamma}_{l\sigma,1}. \end{aligned} \quad (\text{B14})$$

In this equation, all terms with a product of 2 Majorana operators correspond to the one-electron terms, while terms with 4 Majorana operators correspond to two-electron terms. This representation thus allows for the analytical separation of the one-electron terms that are present in the two-electron tensor. Finally, we note that each resulting Majorana product will map to an individual Pauli product when using fermion to qubit mappings such as Jordan-Wigner or Bravyi-Kitaev.

### Appendix C: Finding the optimal symmetry shift for 1-norm minimization

In this section we present procedures for finding the efficient vector associated with the symmetry shift procedure in Sec. IID, both for the one- and two-electron cases.

#### 1. Two-electron symmetry reduction

For finding the symmetry shift of two-electron operators, we here present a linear programming routine that minimizes the 1-norm and is computationally efficient. Since the 1-norm of an arbitrary two-electron operator depends on the unitarization method, we minimize an approximate 1-norm instead for computational efficiency, corresponding to  $\sum_{ij} |\tilde{g}_{ijij}|$  for an operator as seen in Eq.(1).

Our 1-norm minimization routine can be written for arbitrary occupation number polynomial symmetries corresponding to  $\hat{H} - \sum_u s_u \hat{S}_u$ , which can be written as

$$\min_{\vec{s}} \sum_{\nu=1}^{|\mathcal{C}|} |\lambda_{\nu} - \sum_{u=1}^{|\mathcal{S}|} s_u \tau_{\nu}^{(u)}|. \quad (\text{C1})$$

In the above equation, vector  $\vec{\lambda}$  collects the diagonal elements of the two-electron tensor that appear in the array of Cartan operators  $C = \{\hat{n}_p \hat{n}_q \mid p \geq q\} \equiv \{\hat{C}_{\nu} \mid \nu = 1, \dots, |\mathcal{C}|\}$ . The vectors we use for this notation run over  $p \geq q$  in the same order as  $C$ , with the number of elements  $|\mathcal{C}| = n(n+1)/2$ . This also defines the  $\vec{\tau}^{(u)}$  vectors, which represent the symmetry operators:  $\hat{S}_u = \sum_{\nu=1}^{|\mathcal{C}|} \tau_{p,q}^{(u)} \hat{C}_{\nu}$ . As outlined in the main text, the only symmetry that we consider for the two-electron component is  $\hat{N}_e^2$ , which corresponds to  $\tau_{pq} = 1, \forall p, q$ . However, we outline the linear programming routine for arbitrary symmetry operator pools.

We used a linear programming technique to find  $\vec{s}$  efficiently while directly minimizing the 1-norm. To this end, we need to transform the sum of absolute values in the 1-norm cost function into a sum of linear parameters. We achieve this by introducing a new set of auxiliary parameters equivalent to the absolute value functions that appear in the 1-norm. The minimization procedure is subject to constraints that satisfy the absolute value conditions. For the 1-norm linearization, let us begin with introducing the auxiliary vector  $\vec{t}$  and re-write the objective function as

$$\begin{aligned} \min_{\vec{s}} \sum_{\nu} t_{\nu}(\vec{s}) \\ \text{subject to} \quad t_{\nu}(\vec{s}) = \sum_{\nu} |\lambda_{\nu} - \sum_u s_u \tau_{\nu}^{(u)}|. \end{aligned} \quad (\text{C2})$$

The absolute value constraints can be written as

$$\sum_u s_u \tau_{\nu}^{(u)} - \lambda_{\nu} \leq t_{\nu} \quad (\text{C3})$$

and

$$-\sum_u s_u \tau_{\nu}^{(u)} + \lambda_{\nu} \leq t_{\nu} \quad (\text{C4})$$

We can now write the final form for the 1-norm minimization problem:

$$\begin{aligned} \min_{\{\vec{s}, \vec{t}\}} \sum_{\nu} t_{\nu} \\ \text{subject to} \quad \begin{pmatrix} \underline{\tau} & -\underline{1} \\ -\underline{\tau} & -\underline{1} \end{pmatrix} \begin{pmatrix} \vec{s} \\ \vec{t} \end{pmatrix} \leq \begin{pmatrix} \vec{\lambda} \\ -\vec{\lambda} \end{pmatrix}, \end{aligned} \quad (\text{C5})$$

where we have defined the matrix  $\underline{\tau}$  such that the product  $(\underline{\tau} \times \vec{s})_{\nu} \equiv \sum_u s_u \tau_{\nu}^{(u)}$ , and the inequality runs over each index  $\nu \in \{1, \dots, |\mathcal{C}|\}$ . The above minimization problem is linear programmable and lets us efficiently find the global minimum of the 1-norm of the objective function. Moreover, the  $\underline{\tau}$  matrix helps to avoid storing in memory the full two-electron tensors of symmetry operators, which reduces the memory demand significantly. We used the high global minimization algorithm [34] for our numerical calculations.

## 2. One-electron symmetry reduction

Here we review the method for finding the optimal symmetry shift minimizing the 1-norm of the one-electron term  $\hat{H}'_1(s_2)$  obtained after including the one-body modification from  $s_2\hat{N}_e^2$  to  $\hat{H}'_1$  [Eq. (27)]. This method optimizes a real number  $s_1$ , such that the resulting 1-norm of the operator  $\hat{H}''_1(s_1, s_2) \equiv \hat{H}'_1(s_2) - s_1\hat{N}_e$  is minimized. Since  $\hat{N}_e$  commutes with orbital rotations,

$$\hat{H}''_1(s_1, s_2) = \hat{U}^\dagger \left( \sum_{i\sigma} \mu_i(s_2) \hat{n}_{i\sigma} \right) \hat{U} - s_1 \hat{N}_e \quad (C6)$$

$$= \hat{U}^\dagger \left( \sum_{i\sigma} (\mu_i(s_2) - s_1) \hat{n}_{i\sigma} \right) \hat{U}, \quad (C7)$$

therefore, minimizing the 1-norm of  $\hat{H}''_1(s_1, s_2)$  is equivalent to minimizing  $\sum_i |\mu_i(s_2) - s_1|$ , which can be done efficiently using linear programming as outlined for the two-body symmetry shift routine.

### Appendix D: Molecular geometries and computational details

In this section we write down all details necessary for numerical reproducibility. Our code is available at <https://github.com/iloaiza/MAMBO>.

For the CSA decompositions of the two-electron tensor, the cost function was chosen as the 2-norm of  $\Delta\hat{H} \equiv$

$$\sum_{\sigma\sigma'} \sum_{ijkl} b_{ijkl} \hat{E}_{j\sigma}^{i\sigma'} \hat{E}_{l\sigma'}^{k\sigma}:$$

$$\|\Delta\hat{H}\|_2 \equiv \sum_{ijkl} |b_{ijkl}|^2, \quad (D1)$$

considering the decomposition finished when this norm is below a tolerance of  $1 \times 10^{-6}$ . All non-linear optimizations were done using the Julia Optim.jl package [35], using the BFGS algorithm [36] with the default tolerance. Linear programming routines were done using the Julia JuMP package [37] with the HiGHS optimizer [34].

### 1. Molecular Hamiltonians

All molecular Hamiltonians were generated using the PySCF package [38–40] and the Openfermion library [41], using a minimal STO-3G basis [5, 42] and the Jordan-Wigner transformation [27]. The nuclear geometries for the Hamiltonians are:

- R(H – H) = 1Å for H<sub>2</sub>
- R(Li – H) = 1Å for LiH
- R(Be – H) = 1Å with a collinear atomic arrangement for BeH<sub>2</sub>
- R(O – H) = 1Å with angle  $\angle\text{HOH} = 107.6^\circ$  for H<sub>2</sub>O
- R(N – H) = 1Å with  $\angle\text{HNN} = 107^\circ$  for NH<sub>3</sub>

- 
- [1] Y. Cao, J. Romero, J. P. Olson, M. Degroote, P. D. Johnson, M. Kieferová, I. D. Kivlichan, T. Menke, B. Peropadre, N. P. D. Sawaya, et al., *Chem. Rev.* **119**, 10856 (2019), URL <https://doi.org/10.1021/acs.chemrev.8b00803>.
- [2] I. Kassal, S. P. Jordan, P. J. Love, M. Mohseni, and A. Aspuru-Guzik, *Proc. Natl. Acad. Sci.* **105**, 18681 (2008), URL <https://www.pnas.org/doi/abs/10.1073/pnas.0808245105>.
- [3] D. S. Abrams and S. Lloyd, *Phys. Rev. Lett.* **83**, 5162 (1999), URL <https://link.aps.org/doi/10.1103/PhysRevLett.83.5162>.
- [4] A. Y. Kitaev, arXiv (1995), URL <https://arxiv.org/abs/quant-ph/9511026>.
- [5] A. Szabo and N. Ostlund, *Modern Quantum Chemistry: Introduction to Advanced Electronic Structure Theory*, Dover Books on Chemistry (Dover Publications, 1996), ISBN 9780486691862, URL <https://books.google.ca/books?id=k-DcCgAAQBAJ>.
- [6] E. van der Berg and K. Temme, *Quantum* **4**, 322 (2020), URL <https://doi.org/10.22331/q-2020-09-12-322>.
- [7] M. Suzuki, *J. Math. Phys.* **32**, 400 (1991), URL <https://doi.org/10.1063/1.529425>.
- [8] D. W. Berry, C. Gidney, M. Motta, J. McClean, and R. Babbush, *Quantum* **3**, 208 (2019), URL <https://doi.org/10.22331/q-2019-12-02-208>.
- [9] V. von Burg, G. H. Low, T. Haner, D. Steiger, M. Reiher, M. Roetteler, and M. Troyer, *Phys. Rev. Research* **3**, 033055 (2020), URL <https://doi.org/10.1103/PhysRevResearch.3.033055>.
- [10] J. Lee, D. W. Berry, C. Gidney, W. J. Huggins, J. R. McClean, N. Wiebe, and R. Babbush, *PRX Quantum* **2**, 3 (2021), URL <https://doi.org/10.1103/2Fprxquantum.2.030305>.
- [11] A. M. Childs and N. Wiebe, *Quantum Info. Comput.* **12**, 901–924 (2012), ISSN 1533-7146, URL <https://dl.acm.org/doi/10.5555/2481569.2481570>.
- [12] E. Campbell, *Phys. Rev. Lett.* **123**, 070503 (2019), URL <https://link.aps.org/doi/10.1103/PhysRevLett.123.070503>.
- [13] I. D. Kivlichan, C. E. Granade, and N. Wiebe, arXiv (2019), URL <https://arxiv.org/abs/1907.10070>.
- [14] A. M. Childs, Y. Su, M. C. Tran, N. Wiebe, and S. Zhu, *Phys. Rev. X* **11**, 011020 (2021), URL <https://link.aps.org/doi/10.1103/PhysRevX.11.011020>.
- [15] J. Haah, M. B. Hastings, R. Kothari, and G. H. Low, *SIAM J. Comput.* pp. FOCS18–250 (2021), URL <https://epubs.siam.org/doi/10.1137/18M1231511>.

- [16] G. H. Low and N. Wiebe, *Hamiltonian simulation in the interaction picture* (2019), 1805.00675.
- [17] E. Koridon, S. Yalouz, B. Senjean, F. Buda, T. E. O'Brien, and L. Visscher, *Phys. Rev. Research* **3**, 033127 (2021), URL <https://doi.org/10.1103/2Fphysrevresearch.3.033127>.
- [18] A. Dong, D. Fang, and L. Lin, *Quantum* **5**, 459 (2021), URL <https://doi.org/10.22331/q-2021-05-26-459>.
- [19] A. Dong, D. Fang, and L. Lin, *Quantum* **6**, 690 (2022), URL <https://doi.org/10.22331/q-2022-04-15-690>.
- [20] A. F. Izmaylov, T.-C. Yen, R. A. Lang, and V. Verteletskiy, *J. Chem. Theor. Comput.* **16**, 190 (2020), URL <https://doi.org/10.1021/acs.jctc.9b00791>.
- [21] O. Crawford, B. van Straaten, D. Wang, T. Parks, E. Campbell, and S. Brierley, *Quantum* **5**, 385 (2021), URL <https://doi.org/10.22331/2Fq-2021-01-20-385>.
- [22] T.-C. Yen and A. F. Izmaylov, *PRX Quantum* **2**, 4 (2021), ISSN 2691-3399, URL <http://dx.doi.org/10.1103/PRXQuantum.2.040320>.
- [23] D. W. Berry, A. M. Childs, Y. Su, X. Wang, and N. Wiebe, *Quantum* **4**, 254 (2020), URL <https://doi.org/10.22331/q-2020-04-20-254>.
- [24] D. W. Berry, A. M. Childs, R. Cleve, R. Kothari, and R. D. Somma, *Phys. Rev. Lett.* **114**, 090502 (2015), URL <https://link.aps.org/doi/10.1103/PhysRevLett.114.090502>.
- [25] G. H. Low and I. L. Chuang, *Quantum* **3**, 163 (2019), URL <https://doi.org/10.22331/q-2019-07-12-163>.
- [26] A. Gilyén, Y. Su, G. H. Low, and N. Wiebe, in *Proc. 51st ACM SIGACT Theor. Comput.* (2019), pp. 193–204, URL <https://doi.org/10.1145/3313276.3316366>.
- [27] E. Wigner and P. Jordan, *Z. Phys* **47**, 631 (1928), URL [https://ui.adsabs.harvard.edu/link\\_gateway/1928ZPhy...47..631J/doi:10.1007/BF01331938](https://ui.adsabs.harvard.edu/link_gateway/1928ZPhy...47..631J/doi:10.1007/BF01331938).
- [28] S. B. Bravyi and A. Y. Kitaev, *Ann. Phys.* **298**, 210 (2002), URL <https://doi.org/10.1006/aphy.2002.6254>.
- [29] J. T. Seeley, M. J. Richard, and P. J. Love, *J. Chem. Phys.* **137**, 224109 (2012), URL <https://doi.org/10.1063/1.4768229>.
- [30] A. Tranter, S. Sofia, J. Seeley, M. Kaicher, J. McClean, R. Babbush, P. V. Coveney, F. Mintert, F. Wilhelm, and P. J. Love, *Int. J. Quantum Chem.* **115**, 1431 (2015), URL <https://doi.org/10.1002/qua.24969>.
- [31] A. Tranter, P. J. Love, F. Mintert, and P. V. Coveney, *J. Chem. Theor. Comput.* **14**, 5617 (2018), URL <https://doi.org/10.1021/acs.jctc.8b00450>.
- [32] A. F. Izmaylov and T.-C. Yen, *Quantum Sci. Tech.* **6**, 4 (2021), ISSN 2058-9565, URL <http://dx.doi.org/10.1088/2058-9565/ac1040>.
- [33] J. Watkins, N. Wiebe, A. Roggero, and D. Lee, arXiv preprint arXiv:2203.11353 (2022), URL <https://arxiv.org/abs/2203.11353>.
- [34] Q. Huangfu and J. Hall, *Math. Prog. Comput.* **10** (2018), URL <https://doi.org/10.1007/s12532-017-0130-5>.
- [35] P. K. Mogensen and A. N. Riseth, *J. Open Source Softw.* **3**, 615 (2018), URL <https://doi.org/10.21105/joss.00615>.
- [36] R. Fletcher, *Practical Methods of Optimization* (Wiley, 2013), ISBN 9781118723180, URL [https://books.google.ca/books?id=\\_WuAvIx0EE4C](https://books.google.ca/books?id=_WuAvIx0EE4C).
- [37] I. Dunning, J. Huchette, and M. Lubin, *SIAM Review* **59**, 295 (2017).
- [38] Q. Sun, *J. Comput. Chem.* **36**, 1664 (2015), URL <https://onlinelibrary.wiley.com/doi/abs/10.1002/jcc.23981>.
- [39] Q. Sun, T. C. Berkelbach, N. S. Blunt, G. H. Booth, S. Guo, Z. Li, J. Liu, J. D. McClain, E. R. Sayfutyarova, S. Sharma, et al., *WIREs Comput. Mol. Sci.* **8**, e1340 (2018), URL <https://wires.onlinelibrary.wiley.com/doi/abs/10.1002/wcms.1340>.
- [40] Q. Sun, X. Zhang, S. Banerjee, P. Bao, M. Barbry, N. S. Blunt, N. A. Bogdanov, G. H. Booth, J. Chen, Z.-H. Cui, et al., *J. Chem. Phys.* **153**, 024109 (2020), URL <https://doi.org/10.1063/5.0006074>.
- [41] J. R. McClean, N. C. Rubin, K. J. Sung, I. D. Kivlichan, X. Bonet-Monroig, Y. Cao, C. Dai, E. S. Fried, C. Gidney, B. Gimby, et al., *Quantum Sci. Tech.* **5**, 034014 (2020), URL <https://doi.org/10.1088/2058-9565/ab8ebc>.
- [42] W. J. Hehre, R. F. Stewart, and J. A. Pople, *J. Chem. Phys.* **51**, 2657 (1969), URL <https://doi.org/10.1063/1.1672392>.
- [43] Representing the Hamiltonian using only excitation operators is usually referred to as chemists' notation. This entails a modification to the one-electron tensor with respect to physicists' notation, which uses normal-ordered operators of the form  $\hat{a}_p^\dagger \hat{a}_q^\dagger \hat{a}_r \hat{a}_s$ . Our notation is related to the electronic integrals by  $\tilde{g}_{ijkl} = \frac{1}{2} \int \int d\vec{r}_1 d\vec{r}_2 \frac{\phi_i^*(\vec{r}_1) \phi_j(\vec{r}_1) \phi_k(\vec{r}_2) \phi_l^*(\vec{r}_2)}{|\vec{r}_1 - \vec{r}_2|}$  and  $\tilde{h}_{ij} = -\sum_k \tilde{g}_{ikkj} + \int d\vec{r} \phi_i^*(\vec{r}) \left( -\frac{\nabla^2}{2} - \sum_n \frac{Z_n}{|\vec{r} - \vec{r}_n|} \right) \phi_j(\vec{r})$ , with  $\phi_i(\vec{r})$  the one-particle electronic basis functions, and  $Z_n/\vec{r}_n$  the charge/position of nucleus  $n$ .